ACS Medicinal Chemistry Letters

Letter

Discovery of novel neuraminidase inhibitors by structure-based virtual screening, structural optimization, and bioassay

Rao Yu, Li Ping Cheng, Meng Li, and Wan Pang

ACS Med. Chem. Lett., **Just Accepted Manuscript** • DOI: 10.1021/acsmedchemlett.9b00447 • Publication Date (Web): 25 Nov 2019

Just Accepted

is published by the American Chemical Society. 1155 Sixteenth Street N.W., Washington, DC 20036

Discovery of novel neuraminidase inhibitors by structure-based virtual screening, structural optimization, and bioassay

Rao Yu, Li Ping Cheng*, Meng Li, Wan Pang

*School of Chemical and Environmental Engineering, Shanghai Institute of Technology, Shanghai 201418, China

KEYWORDS: Virtual screening; neuraminidase; inhibitors; bioassay.

ABSTRACT: Neuraminidase (NA) is a significant therapeutic target for treating influenza. In this study, a new lead NA inhibitor **AN-329/10738021** was discovered by structure-based virtual screening, molecular dynamics simulations, and bioassay validation. Optimization of lead **AN-329/10738021**, which holds a novel scaffold of N'-benzylidene benzohydrazone, leads to discovery of some novel NA inhibitors **Y-1**-**Y-11**. Compound **Y-1** exerts the best inhibition activity (IC_{50}=0.21 μM) against NA, which is better than oseltamivir carboxylate (OSC) (IC_{50} =3.04 μM) and lead **AN-329/10738021** (IC_{50} =1.92 μM). Molecular docking analysis indicates that the good potency of **Y-1** may be ascribed to the elongation of benzylidene moiety of the molecule to the 430-cavity. The results of this study may offer useful reference for development of novel NA inhibitors.

Influenza virus belongs to the *Orthomyxoviridae* family. It can be classified as four types (A, B, C and D) according to the antigenicity of nucleoprotein. As the main pathogen of human influenza, influenza A is often prone to cause influenza outbreak or pandemic. Influenza A virus is an enveloped negative-strand RNA virus. Its genome, which encodes up to 11 proteins, comprises eight viral RNA (vRNA) segments (PB2, PB1, PA, HA, NP, NA, M, and NS). [1-2] The base of single-stranded RNA is unstable and more likely to mutate than double-stranded. What's more, gene exchange, deletion and addition may occur between different eight RNA segments, which may lead to gene recombination. Therefore, the development of highly efficient anti-influenza drugs, which are insusceptible to virus mutation, is particularly important.

Neuraminidase (NA), a surface glycoprotein in influenza virus, plays crucial rule in viral replication and infection and is a validated target for design of anti-influenza drugs.[3-4] Currently, the first-choice anti-influenza drugs recommended for treating influenza virus are NA inhibitors, such as oseltamivir and zanamivir.[5] Though these antiviral drugs are efficient against the current influenza virus strains, their use can lead to the occurrence of drug-resistant virus.[6]

Recently, a new pocket named "430-cavity", which is adjacent to the active site of the NA, attracts great attention. 430-cavity has large molecular volume and connects directly to active site, which makes it a promising binding site for inhibitor design. What's more, 430-cavity widely exists in various subtypes of influenza virus, and NA inhibitors designed based on 430-cavity have broad spectrum.[7] Some research groups have designed some new NA inhibitors based on 430-cavity, and have achieved good results. For example, Ju *et al*.[7] had discovered a series of novel oseltamivir derivatives targeting the 430-cavity. Zhu *et al*.[8] had designed and synthesized a series of novel analogues of zanamivir as NA inhibitors. The good inhibitory activity may be ascribed to the elongation of the C-1- groups of the molecules to the 430-cavity.

In this research, the discovery of novel NA inhibitors was performed by structure-based virtual screening, molecular dynamics (MD) simulations, chemical synthesis and bioassay. A novel lead compound was firstly hit by virtual screening, then the lead compound was used as template to design some new NA inhibitors targeting the 430-cavity. Finally, the designed 11 new inhibitors were synthesized and tested for biological activity.

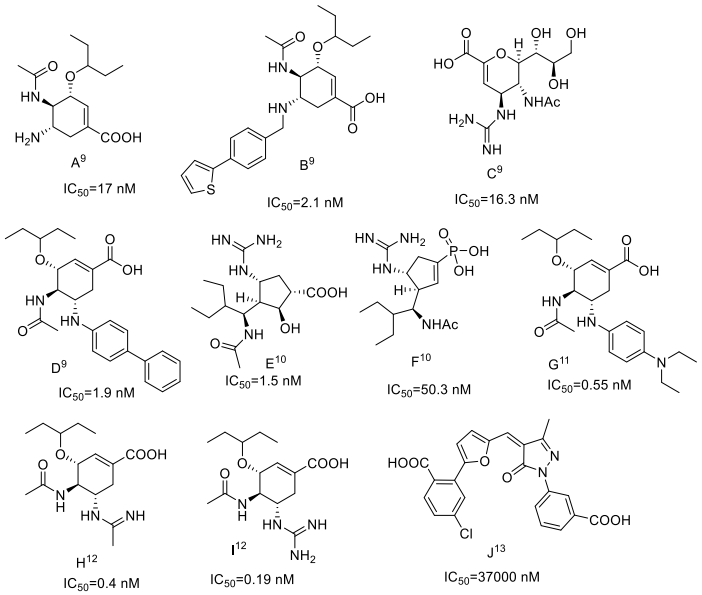

Figure 1. Structures of representative NA inhibitors

In this paper, 10 typical NA inhibitors (shown in Fig.1) were picked out to generate pharmacophore models from different references.[9-13] And the pharmacophore models were constructed by GALAHAD module of SYBYL-X 2.1 package (Tripos Inc. St. Louis, USA). The obtained 20 pharmacophoric models were validated by performing Güner-Henry (GH) test.[14] The GH test set contains 78 active molecules and 100 inactive molecules. The best pharmacophoric model hits a total of 79 molecules in

the GH test set, which includes 76 active and 3 inactive molecules. The GH test score was 0.94, a threshold value considered as an excellent model, implying that this pharmacophoric model can be used to screening.[15-17] The detailed statistical parameters are shown in Table 1.

Table 1. The detailed statistical parameters of the best pharmacophore model based on the GH Test

parameters	value
total molecules in test set (D)	178
total number of actives in test set (A)	78
total hits (Ht)	79
active hits (Ha)	76
%Y, yield of actives [(Ha /Ht) × 100]	96.2
% A, ratio of actives [(Ha /A) × 100]	97.4
enrichment factor (EF) [a]	2.20
GH test score [b]	0.94

[a] EF = (Ha D)/(Ht A). [b] GH test score = [Ha (3A + Ht)/(4Ht A)][1 -(Ht - Ha)/(D - A)].

The characteristics of the best pharmacophoric model was shown in Fig. 2, including two positive nitrogen (NP_2, NP_3), two donor atoms (DA_1, DA_4), two hydrophobic centers (HY-7, HY-8), two acceptor atoms (AA-5, AA_6), and one negative center (NC_9). As seen from Fig. 2A, the known inhibitor **I** (Fig. 1) was superimposed on the pharmacophoric features. The carboxyl of inhibitor **I** can be readily superimposed on negative center (NC_9) and H-bond acceptor (AA_5). Cyclohexene ring was superimposed on hydrophobic center (HY_7). The aliphatic chain moiety of 3-(1-ethylpropoxy) makes it one hydrophobic center (HY_8). The carbonyl group of acetylamino was superimposed on H-bond acceptor (AA_6). The two imino nitrogens of guanidyl could be readily identified by features of NP_2 and NP_3, respectively.

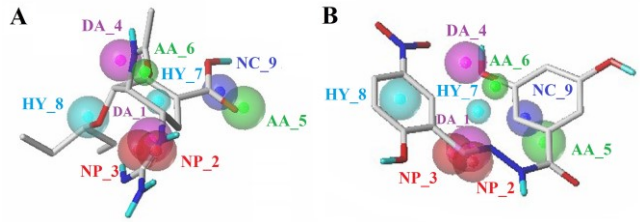

Figure 2. Alignment known inhibitors **I**(A) and lead compound **AN-329/10738021**(B) on derived pharmacophoric features.

The workflow of virtual screening in this study is displayed in **Fig. 3**. The large SPECS database, consisting of 212,713 small molecules, was selected for virtual screening in this work. The best pharmacophoric model was used as a 3D query to screen the SPECS database using the UNITY search engine in SYBYL-X 2.1. 1024 molecules were hit. The Lipinski drug five principles were used as filters to screen the drug properties of the compound, and finally **Database 2** (774 compounds) were obtained.

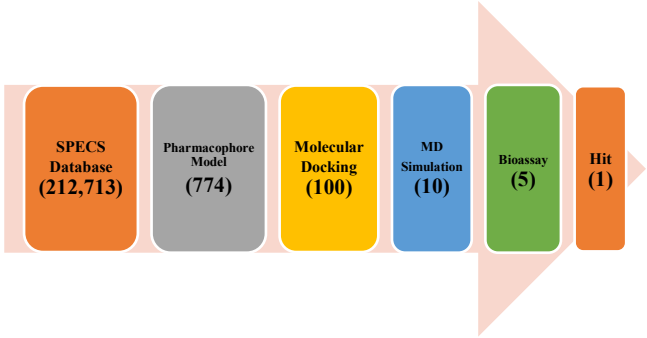

Figure 3. Workflow of the virtual screening process.

Subsequently, molecular docking[18] had been carried out for **Database 2** to study the binding modes between inhibitors and NA crystal structures (PDB ID: 2HU0). As a result, the top 100 compounds with higher docking scores and binding modes close to that of the original extracted ligand with 2HU0 were screened out to compose **Database 3**. By carefully analysis of the spatial matching and interactions between the 100 compounds and NA protein, 10 compounds with higher total score values were selected to form **Database 4** for further study. The structures of the 10 compounds are shown in Fig. 4 (**SPECS-1-SPECS-5**) and Fig. S1 (**SPECS-6-SPECS-10**).

To discovery of novel lead compounds, MD simulations were performed for 10 compounds in **Database 4** by Amber 12.[19] The stability of the NA-inhibitor complex was determined based on the root-mean-square deviation (RMSD)[20] values of the acceptor backbone atoms (Fig. S2 and Fig. S3). The results show that five compounds can well embed in the active site or 430-cavity of the neuraminidase and have smaller binding energies compared with the other five compounds. The predicted binding free energies (ΔG_{bind}) of the 10 compounds via Molecular Mechanics/Generalized Born Surface Area (MM/GBSA)[21] and Molecular Mechanism/Poison-Boltzman Surface Area (MM/PBSA)[22] methods are listed in Table S1 and Table S2. It is known that there is generally a good correlation between binding free energy and compound's activity. The more negative the ΔG_{bind} of compound is, the more active the compound is.[21,22] By calculation of the binding free energies of the 10 compounds in **Database 4**, and **5** compounds (**SPECS-1-SPECS-5**) with smaller binding free energies were selected to make up **Database 5**.

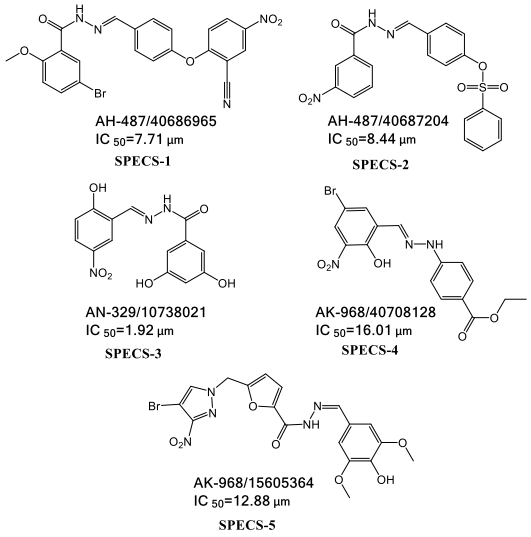

Figure 4. Chemical structures and inhibitory activity of the five NA inhibitors with their SPECS IDs.

Then, the 5 compounds in **Database 5** were bought from SPECS for further biological evaluation. OSC was selected as the reference compound. The results show that five compounds all exert good potency, with IC_{50} values of less than 20 μM (Fig. 4), Compound **AN-329/10738021** has the best inhibitory activity (IC_{50}=1.92 μM), which is better than OSC (IC_{50} =3.04 μM). Moreover, among the five compounds, three compounds (**AN-329/10738021**, **AH-487/40686965**, and **AH-487/406867204**) with the lowest IC_{50} values all have the same skeleton structure of N'-benzylidene benzohydrazone. Accordingly, compound **AN-329/10738021** could be used as a lead compound to perform further modification to obtain new inhibitors with good inhibition activity. As shown in Fig. 2B, lead compound **AN-329/10738021** was superimposed onto the pharmacophoric features. Compared with the features in Fig. 2A, the 3,5-dihydroxy substituted benzohydrazide makes the C-1 and C-2 position one acceptor center (AA_5) and negative center (NC_9). Two positive nitrogen atoms of -C=N-NH- group could be readily identified by features of NP-2 and NP-3. The 5-nitrobenzylidene can be readily superimposed on hydrophobic (HY_8) center. Consequently, the lead compound was valuable for further study for its good inhibitory activity.

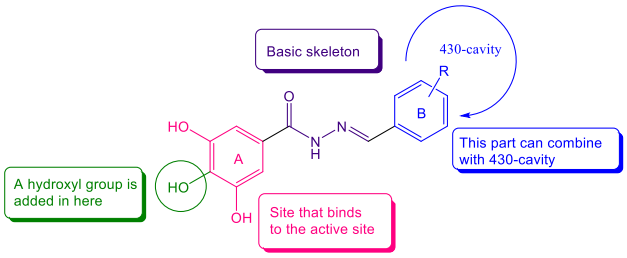

Figure 5. The design of new inhibitors based on the lead compound.

According to the features derived from the pharmacophoric model and molecular docking results, some new NA inhibitors (**Y-1-Y-11**) were designed (**Table 2** and **Scheme 1**). Lead compound **AN-329/10738021** was used as template. The design idea was summarized in Fig. 5. 430-cavity is mainly composed of Trp403, Lys432, Ile427 and Thr439 etc, which could be regarded as a hydrophobic pocket. Therefore, some hydrophobic groups, such as nitro groups (**Y-1-Y-4**) and methoxy groups (**Y-5, Y-6**), were introduced to ring B expected to interact with 430-cavity. It was revealed that the active site of NA could be empirically divided into 5 regions, termed subsites S1-S5, that are essential for the interactions with different NA inhibitors (Fig. 6).[23] S1 site consists of three positively charged arginine residues (Arg118, Arg292 and Arg371), which can form very strong electrostatic interactions with anionic substituents from the inhibitor and provide hydrogen-bonding environment. S2 site is comprised of Glu119 and Glu227, which can form hydrogen bonds with basic groups. S3 site is a small hydrophobic region formed by the side chains of Trp 178 and Ile 222 adjacent to a polar region provided by the side chain of Arg 152, which can interact with various hydrophobic groups; S4 site is a hydrophobic region comprised of side chains of Ile 222, Ala 246, and the hydrophobic face of Arg 224, which also can interact with some hydrophobic groups. S5 is a mixed polarity region formed from the carboxylate of Glu 276 and the methyl of Ala 246, which may produce interactions with various groups by the hydrophilic carboxyl of Glu276 and the hydrophobic methyl of Ala246. The flexible 430-cavity is next to the subsite S1,[8] which can provide a large cavity adjacent to the active site. This provides a good chance to design highly novel NA inhibitors that target both the 430-cavity and the known active subsites. Herein we designed and synthesized a series of lead compound analogs (**Y-1-Y11**) with different substitutions at aryl B rings to explore the 430-cavity.

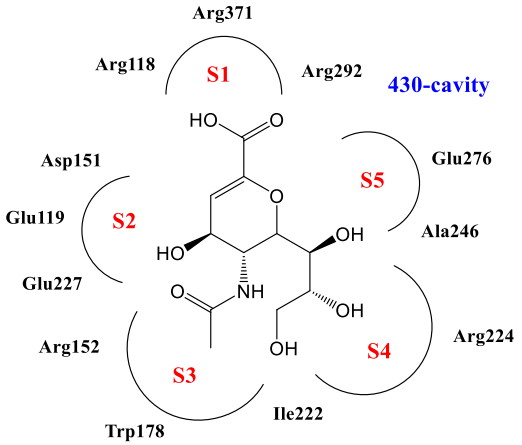

Figure 6. Schematic diagram of S1-S5 sites division and binding mode of NA and sialic acid.[23]

Table 2. Activity of the Compounds Y-1-Y-11 in the Bioassay against NA

Compd	IC_{50}(μM)	Compd	IC_{50}(μM)
Y-1	0.21±0.04	**Y-7**	13.77±2.89
Y-2	3.71±0.53	**Y-8**	9.67 ±1.33
Y-3	5.47±1.32	**Y-9**	10.56 ±1.89
Y-4	3.97 ±0.55	**Y-10**	22.74±3.55
Y-5	14.83 ±3.76	**Y-11**	36.60±4.17
Y-6	11.64 ±2.41	OSC	3.04±0.47
Lead[a]	1.92 ±0.41		

[a]*Lead is **AN-329/10738021**.*

Compounds **Y-1-Y-11** were synthesized by feasible synthetic strategies in Scheme 1. Their activities against NA were further biologically tested. The inhibitory profiles for in vitro tests are displayed in Fig. S4. For comparison, lead compound **AN-329/10738021** and OSC were evaluated as the reference compounds. As seen from Table 2, Compound **Y-1** exhibits the most potent inhibitory activity (IC_{50} =0.21 μM), which is better than **AN-329/10738021** (IC_{50} =1.92 μM) and OSC (IC_{50} =3.04 μM). The activities of **Y-2** (IC_{50} =3.71 μM), **Y-3** (IC_{50} =5.47 μM) and **Y-4** (IC_{50} =3.97 μM) are comparable to that of OSC. It can be seen that compounds with strongly electronegative groups (such as nitro group and halogen atoms) in ring B show better inhibitory activity, whereas the introduction of methoxy and amide groups (**Y-5-Y-7**) in ring B maybe decrease the compounds' activity. As shown in Scheme 1, the only difference between **Y-1-Y-4** and **Y-8-Y-11** is the existence of an additional hydroxy group at the para-position of hydrazone group, which decreases compounds' activity. This trend could be rationalized with the strong hydrophilicity of hydroxy group. Molecular docking analysis indicates that the hydroxyl group of A ring at the para-position of hydrazone group is close to S3 or S4 region of the NA active site (see Fig. S5). Nevertheless, S3 and S4 are hydrophobic regions, which interact with hydrophobic groups well.

To better comprehend the differentiation of inhibitory activity of **Y-1**, **AN-329/10738021**, and OSC, molecular docking was carried out to study the binding modes between NA and inhibitors. Fig. 7 shows the binding poses of **Y-1**, **AN-329/10738021**

and OSC with NA (PDB 2HU0). The 3D figures of **Y-1**, lead compound (**AN-329/10738021**) and OSC had been aligned in Fig. 8 to ensure that protein conformation is the same for all three complexes. From Figures 7 and 8 it can be seen that the rings A of **Y-1** and **AN-329/10738021**, as well as the whole skeleton of OSC can all well implant into the active site of neuraminidase. However, it is worth noting that the aryl B rings in **Y-1** and **AN-329/10738021** could be elongated into the 430-cavity, whereas the OSC could not reach 430-cavity.

From 2D figures one can see that the aryl B rings of **Y-1** and **AN-329/10738021** were projected toward the 430-cavity to form hydrogen bonds and hydrophobic interactions. For example, for **Y-1**, the 3-nitro may form two hydrogen bonds with residue Arg428 of 430-cavity. The 4-hydroxyl can form one hydrogen bond with residue Glu425. The aryl B ring can form extensive hydrophobic interactions with some key residues Ile427, Pro431, and Lys 432 of 430-cavity. For the lead **AN-329/10738021**, the aryl B ring may form hydrophobic interactions with residues Ile427 and Pro431 of 430-cavity. The 5-nitro may form three hydrogen bonds with residues Arg118 and Arg371 of S1 site. Therefore, the good inhibition activity of **Y-1** and lead **AN-329/10738021** may be attributed to their elongated aryl B ring groups. The A ring moiety of **Y-1** and **AN-329/10738021** can also interact with some active region of NA active site. For example, the 3-hydroxyl of **Y-1** may form one hydrogen bond with the hydrophilic carboxyl of Glu276 of S5 site. The 3-hydroxyl of **AN-329/10738021** may form one hydrogen bond with residue Glu227 of S2 region. The 5-hydroxyl may form three hydrogen bonds with residues Arg156 and Glu119 of S2 site. Regarding the acylhydrazone moiety, for **Y-1**, the carbonyl oxygen atom can form three hydrogen bonds with residues Tyr406, Arg292 and Arg371 of S1 site, the double bond nitrogen can form one hydrogen bond with Arg371; no hydrogen bond is formed with the near residues for the lead **AN-329/10738021**. In addition, the acylhydrazone group can form other extensive interactions, such as van der Waals force and carbon hydrogen bond with the around residues of the active site. Comparison of **Y-1** and **AN-329/10738021**, although the aryl B ring may both interact with the 430-cavity, the introduced group in **Y-1** can enter deeper into the 430-cavity and it can form more hydrogen bonds and stronger hydrophobic interactions with the residues of 430-cavity, which may lead to its stronger inhibitory activity compared with the lead **AN-329/10738021**. For OSC, the deprotonated carboxyl may form multiple hydrogen bonds with the near residues (Arg118, Arg292, Arg371, and Tyr347). At the same time, it can form strong electrostatic interactions with the three positively charged arginine residues (Arg118, Arg292, Arg371) of S1 site. The carbonyl oxygen atom of acetylamino may form one hydrogen bond with residue Arg152 of S3 site. The cyclohexene ring and the aliphatic chain moiety of 3-(1-ethylpropoxy) may form strong hydrophobic interactions with residues Trp178, Arg224, Ile222 of S3 and S4 sites. Although OSC can well interact with NA active site, the docking results show that it could not interact with the 430-cavity, which perhaps leads to its weaker activity compared with **Y-1** and the lead **AN-329/10738021**.

A

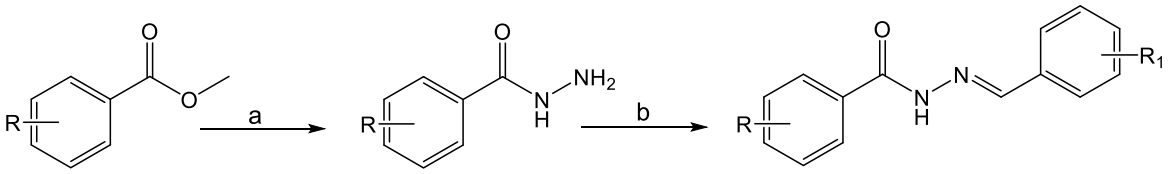

Reagents and conditions: (a) hydrazine hydrate, rt, 24h;(b) aldehyde, rt, 4-6h.

B

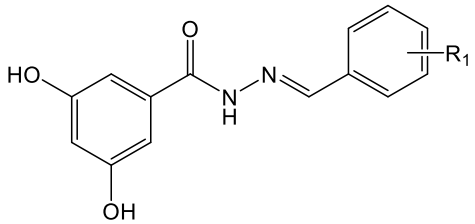

R_1=3-nitro,4-hydroxyl (**Y-1**)
R_1=2-nitro,5-chlorine (**Y-2**)
R_1=3-nitro,4-flurine (**Y-3**)
R_1=2-flurine,5-nitro (**Y-4**)
R_1=3,5-dimethoxy,4-hydroxyl (**Y-5**)
R_1=3-methoxy,4-hydroxyl (**Y-6**)
R_1=4-N-acetylamino (**Y-7**)

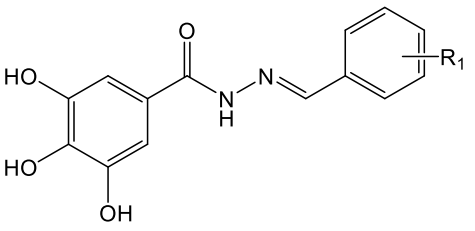

R_1=3-nitro,4-hydroxyl (**Y-8**)
R_1=2-nitro,5-chlorine (**Y-9**)
R_1=3-nitro,4-flurine (**Y-10**)
R_1=2-flurine,5-nitro (**Y-11**)

Scheme 1. Synthesis of Compounds Y-1-Y-11

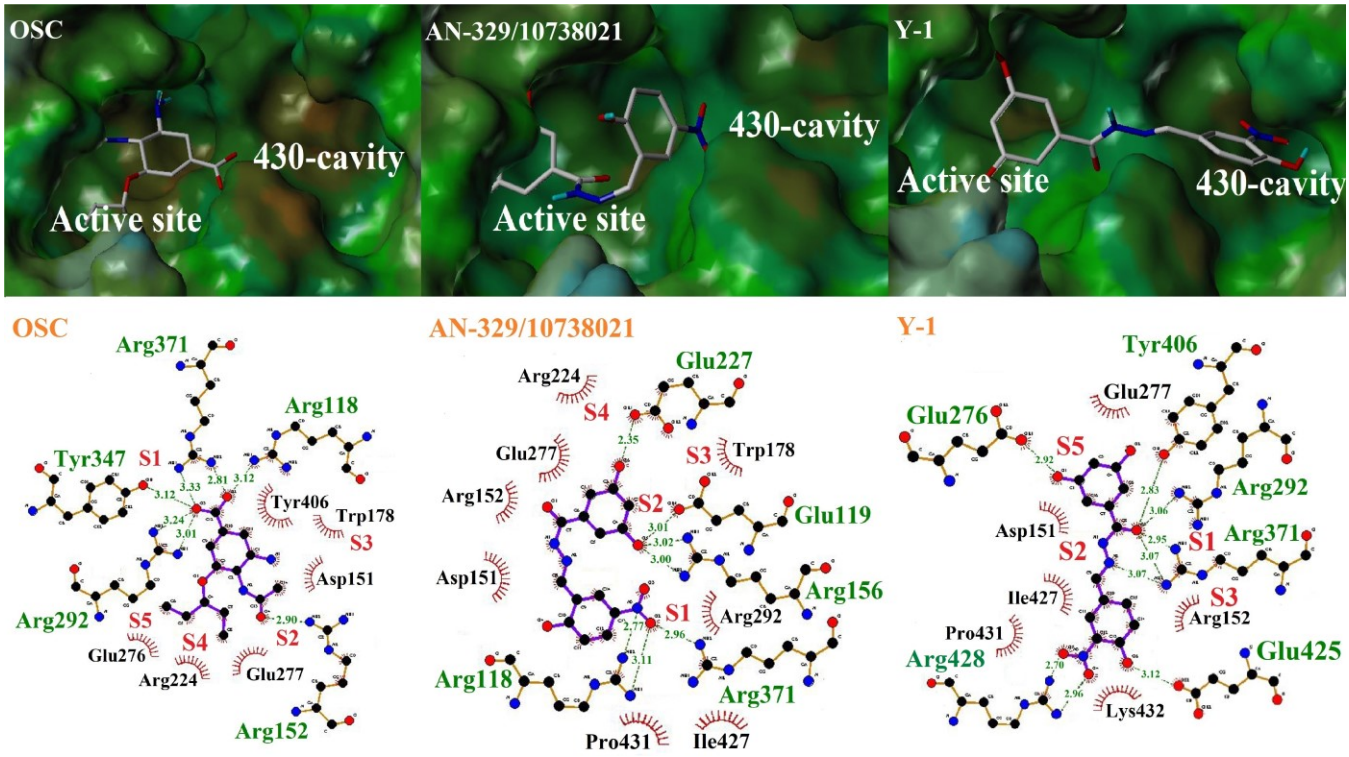

Figure 7. Binding modes of **OSC, AN-329/10738021** and **Y-1** with NA (PDB 2HU0). Hydrogen bonds are indicated by green dotted lines (for the hydrophobic surfaces on protein, brown represents the maximum hydrophobic, and blue represents the maximum hydrophilic).

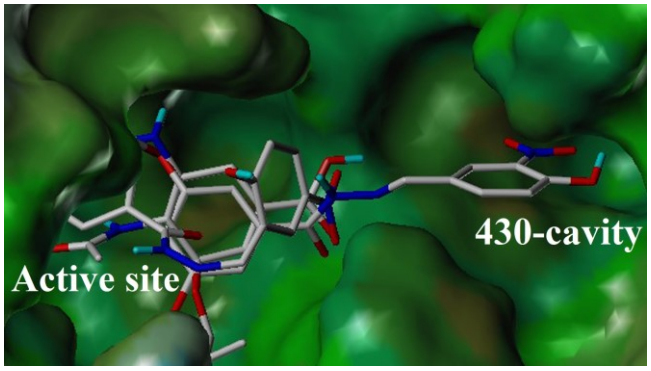

Figure 8. Proposed binding modes of **Y-1**, **AN-329/10738021** and OSC in the active site of NA (PDB 2HU0).

MD simulations were also carried out for all synthesized compounds. The stability of the NA-inhibitor complex was determined based on the RMSD values of the acceptor backbone atoms (Fig. S6). On the base of MD simulations, the binding free energies (ΔG_{bind}) between the 11 new inhibitors and NA were calculated and shown in Table 3. In this research, ΔG_{bind} was calculated by MM/PBSA and MM/GBSA methods. The PB model is theoretically more rigorous than the GB models, and MM/PBSA is often considered to be naturally superior to MM/GBSA in predicting binding free energies.[24] As can be seen from Tables 2 and 3, the smaller the ΔG_{bind} of inhibitor-NA is, the stronger the activity of the inhibitor is for most inhibitors. For example, **Y-1** has the lowest ΔG_{bind} (-31.26 kcal·mol^{-1}) and it exerts the best NA-inhibiting activity. What's more, **Y-2** (-27.85 kcal·mol^{-1}), **Y-3** (-21.87 kcal·mol^{-1}) and **Y-4** (-18.41 kcal·mol^{-1}), which have better inhibitory activities, also have lower ΔG_{bind} values. The ΔG_{bind} values of **Y-1**-**Y-3** are all less than -20.00 kcal·mol^{-1}. **Y-5**-**Y-9** have similar inhibitory activities and their IC_{50} values are about 10.00 μM. And their ΔG_{bind} values are between -15.00 and -20.00 kcal·mol^{-1} except **Y-6**. **Y-10** and **Y-11** have poor activity in inhibition of NA, especially **Y-11**, which has the lowest activity (36.60 μM) and the highest binding energy (-13.00 kcal·mol^{-1}). Hence one can see that the theoretical results are consistent with the experimental results.

Table 3. The Calculated Binding Free Energies (ΔG_{bind}, kcal·mol^{-1}) of Ligand-2HU0 Complexes via MM/PBSA and MM/GBSA Methods

No.	IC_{50}(μM)	VDW	EEL	ΔG_{gas}	ΔG_{GB}	ΔG_{SA}	ΔG_{solv}(GB)	ΔG_{bind}(GB)	ΔG_{PB}	ΔG_{SA}	ΔG_{solv}(PB)	ΔG_{bind}(PB)
Lead *	1.92	-36.74	-11.41	-48.04	31.36	-4.36	26.99	-21.05	32.67	-3.67	29.21	-18.83
Y-1	0.21	-38.30	-17.98	-56.28	26.17	-4.60	21.57	-34.71	28.60	-3.58	25.02	-31.26
Y-2	3.71	-34.39	-15.54	-49.93	27.87	-4.09	23.78	-26.15	25.45	-3.37	22.07	-27.85
Y-3	5.47	-30.57	-30.60	-61.17	40.53	-4.48	36.05	-25.12	42.28	-2.98	39.30	-21.87

Y-4	3.97	-40.86	-23.47	-64.33	44.33	-5.16	39.80	-24.52	49.95	-4.03	45.91	-18.41
Y-5	14.83	-29.53	-55.04	-84.57	68.21	-4.24	63.97	-20.60	68.09	-3.01	65.08	-19.49
Y-6	11.64	-42.66	-8.16	-50.82	27.72	-5.33	22.38	-28.44	31.54	-4.03	27.52	-23.21
Y-7	13.77	-35.57	-36.48	-73.05	49.70	-4.60	45.09	-26.96	55.88	-3.23	52.64	-19.41
Y-8	9.67	-28.81	-39.42	-68.23	52.79	-4.07	48.72	-19.51	54.67	-3.27	51.39	-16.84
Y-9	10.56	-27.12	-6.09	-33.21	18.32	-3.05	15.27	-17.94	18.00	-2.66	15.35	-17.87
Y-10	22.74	-29.56	-25.01	-54.58	37.69	-3.70	34.00	-20.58	41.13	-2.90	38.23	-16.34
Y-11	36.60	-21.01	-5.31	-26.32	15.57	-2.39	13.18	-13.14	15.45	-2.13	13.31	-13.00

: Lead is stands for **AN-329/10738021.*

In this research, a novel lead NA inhibitor **AN-329/10738021** (IC_{50}=1.92 μM) was discovered by virtual screening, MD simulations, and bioassay validation. Structural optimization of **AN-329/10738021** leads to discovery of a series of 11 novel inhibitors (**Y-1**-**Y-11**). These inhibitors exhibit good inhibition activity in the range of potency of FDA-approved oseltamivir carboxylate. They have concise chemical structures and are relatively easy to synthesize, with good potential for further improvement by introducing novel moieties and extension of structures. Particularly, compound **Y-1** exerts the best NA-inhibition activity (IC_{50} = 0.21 μM), which is better than OSC (IC_{50} = 3.04 μM). Molecular docking analysis indicates that the good inhibition activity of **Y-1** may be ascribed to the elongation of benzylidene moiety of the molecule to the 430-cavity. 430-cavity plays an important role in discovery of novel NA inhibitors.

ASSOCIATED CONTENT

Supporting Information

Supplementary Information (methods and materials, database preparation, structure-based virtual screening, Table. S1, Table. S2, Figure. S1, Figure. S2, Figure. S3, Figure. S4, Figure. S5, Figure. S6, general procedure for synthesis of novel compounds and in vitro neuraminidase inhibition assay) associated with this article can be found.

The Supporting Information is available free of charge on the ACS Publications website.

AUTHOR INFORMATION

Corresponding Author

*Phone: +86-21-6087-3250. Email: chengliping@sit.edu.cn

Present Addresses

School of Chemical and Environmental Engineering, Shanghai Institute of Technology, Shanghai 201418, China

Author Contributions

The manuscript was finished through contributions of all authors.

Funding Sources

Thanks for financial support by Natural Science Foundation of Shanghai (No. 15ZR1440400), Collaborative Innovation Fund (No. XTCX2016-14), Middle and Youth Teachers Scientific and Technological Talents Developing Fund (No. ZQ 2018-20), Shanghai Municipal Education Commission (Plateau Discipline Construction Program).

Notes

The authors declare that there is no financial/commercial conflict of interest.

ACKNOWLEDGMENT

Authors are thankful to WuXi AppTec for their help in bioassay.

ABBREVIATIONS

NA**,** neuraminidase; OSC, oseltamivir carboxylate; MD, molecular dynamics; GH, Güner-Henry; RMSD, root-mean-square deviation; MM/GBSA, Molecular Mechanics/Generalized Born Surface Area; MM-PBSA, Molecular Mechanism/Poison-Boltzman Surface Area.

REFERENCES

[1] Muramoto, Y.; Takada, A.; Fujii, K.; Noda, T.; Iwatsuki-Horimoto, K.; Watanabe, S.; Horimoto T.; Kida, H.; Kawaoka Y. Hierarchy among viral RNA (vRNA) segments in their Role in vRNA incorporation into influenza A virions. *J. Virol.* **2006**, 80, 2318-2325.

[2] Lamb, R. A.; Krug R. M. Orthomyxoviridae: the viruses and their replication. **2001**, p. 1487-1531. In Knipe D. M. and Howley P. M. (ed.), Fields virology, 4th ed. Lippincott-Raven Publishers, Philadelphia, Pa.

[3] Das, K.; Aramini, J. M., Ma, L. C.; Krug, R. M.; Arnold, E. Structures of influenza A proteins and insights into antiviral drug targets. *Nat. Struct. Mol. Biol.* **2010**, 17, 530-538.

[4]. Stöhr, K. Preventing and treating influenza. *Br. Med. J.* **2003**, 326, 1223-1224.

[5] McCullers, J. A. Antiviral therapy of influenza. *Expert. Opin. Investig. Drugs.* **2005**, 14, 305-312.

[6] Le, Q. M.; Kiso, M.; Someya, K.; Sakai, Y. T.; Nguyen, T. H.; Nguyen, K. H. L.; Pham, N. D.; Ngyen, H. H.; Yamada, S.; Muramoto, Y.; Horimoto, T.; Takada, A.; Goto, H.; Suzuki, T.; Suzuki Y.; Kawaoka, Y. Avian flu: isolation of drug-resistant H5N1 virus. *Nature*. **2005**, 437, 1108.

[7] Ju, H.; Zhang, J.; Sun, Z. S.; Huang, Z.; Qi, W. B.; Huang, B.; Zhan, P.; Liu, X. Y. Discovery of C-1 modified oseltamivir derivatives as potent influenza neuraminidase inhibitors. *Eur. J. Med. Chem*. **2018**, 146, 220-231.

[8] Feng, E. G.; Shin, W. J.; Zhu, X. L.; Li, J.; Ye, D. J.; Wang, J.; Zheng, M. Y.; Zuo, J. P.; No, K. T.; Liu, X.; Zhu, W. L.; Tang, Wei;

Seong, B. L.; Jiang, H. L.; Liu, H. Structure-Based Design and Synthesis of C-1- and C-4-Modified Analogs of Zanamivir as Neuraminidase Inhibitors. *J. Med. Chem.* **2013**, 56, 671-684.

[9] Xie, Y. C.; Xu, D. Q.; Huang, B; Ma, X. L.; Qi, W. B.; Shi, F. Y.; Liu, X. Y.; Zhang, Y. J.; Xu, W. F. Discovery of N-Substituted Oseltamivir Derivatives as Potent and Selective Inhibitors of H5N1 Influenza Neuraminidase. *J. Med. Chem.* **2014**, 57, 8445-8458.

[10] Wang, P. C.; Fang, J. M.; Tsai, K. C.; Wang, S. Y.; Huang, W. I.; Tseng, Y. C.; Cheng, Y. S. E.; Cheng, T. J. R.; Wong, C. H. Peramivir Phosphonate Derivatives as Influenza Neuraminidase Inhibitors. *J. Med. Chem.* **2016**, 59, 5297-5310.

[11] Zhang, J.; Poongavanam, V.; Kang, D. W.; Bertagnin, C.; Lu, H. M.; Kong, X. J.; Ju, H; Lu, X.Y.; Gao, P.; Tian, Y.; Jia, H. Y.; Desta, S.; Ding, X.; Sun, L.; Fang, Z. J.; Huang, B. S.; Liang, X. W.; Jia, R. F.; Ma, X. L.; Xu, W. F.; Murugan, N. A.; Loregian, A.; Huang, B.; Zhan, P.; Liu, X. Y. Optimization of N-Substituted Oseltamivir Derivatives as Potent Inhibitors of Group-1 and -2 Influenza A Neuraminidases, Including a Drug-Resistant Variant. *J. Med. Chem*. **2018**, 61, 6379-6397.

[12] Schade, D.; Kotthaus, J.; Riebling, L.; Kotthaus, J.; Mueller, F. H.; Raasch, W.; Koch, O.; Seidel, N.; Schmidtke, M.; Clement, B. Development of Novel Potent Orally Bioavailable Oseltamivir Derivatives Active against Resistant Influenza A. *J. Med. Chem.* **2014**, 57, 759-769.

[13] Kumar, V.; Chang, C. K.; Tan, K. P.; Jung, Y. S.; Chen, S. H.; Cheng, Y. S. E.; Liang, P. H. Identification, Synthesis, and Evaluation of New Neuraminidase Inhibitors. *Org. Lett*. **2014**, 16, 5060-5063.

[14] Agarwal, A.; Paliwal, S.; Mishra, R.; Sharma, S.; Kumar, D. A.; Tripathi, R.; Gunjan, S. Discovery of a selective, safe and novel antimalarial compound with activity against chloroquine resistant strain of Plasmodium falciparum. *Scientific Reports.* **2015**, 5, 13838.

[15] Boppana, K.; Dubey, P. K.; Jagarlapudi, Sarma A. R. P.; Vadivelan, S.; Rambabu, G. Knowledge based identification of MAO-B selective inhibitors using pharmacophore and structure based virtual screening models. *Eur. J. Med. Chem.* **2009**, 44, 3584-3590.

[16] Vadivelan, S.; Sinha, B. N.; Irudayam, S. J.; Jagarlapudi, Sarma A. R. P. Virtual screening studies to design potent CDK2-cyclin A inhibitors. *J. Chem. Inf. Model.* **2007**, 47, 1526-1535.

[17] Shih, K. C.; Lin, C. Y.; Zhou, J.; Chi, H. C.; Chen, T. S.; Wang, C. C.; Tseng, H. W.; Tang, C. Y. Development of Novel 3D-QSAR Combination Approach for Screening and Optimizing B-Raf Inhibitors in silico. *J. Chem. Inf. Model*. **2011**, 51, 398-407.

[18] Taylor, R. D.; Jewsbury, P. J.; Essex, J. W. A review of protein-small molecule docking methods. *J. Comput. Aid Mol. Des*. **2002**, 16, 151-166.

[19] Case, D. A.; Darden, T.; Cheatham III TE, Simmerling C, Wang, J. M.; Duke, R. E. et al. *AMBER 12*, University of California, San Francisco, **2013**, 1, p3.

[20] Coutsias, E. A.; Seok, C.; Dill, K. A. Using quaternions to calculate RMSD. *J. Comput. Chem*. **2004**, 25, 1849-1857.

[21] Kollman, P. A.; Massova, I.; Reyes, C.; Kuhn, B.; Huo, S. H.; Chong, L.; Lee, M.; Lee, T. S.; Duan, Y.; Wang, W.; Donini, O.; Cieplak, P.; Srinivasan, J.; Case, D. A.; Cheatham, T. E., III. Calculating structures and free energies of complex molecules: combining molecular mechanics and continuum models. *Acc. Chem. Res*. **2000**, 33, 889-897.

[22] Homeyer, N.; Gohlke, H. Free energy calculations by the molecular mechanics Poisson-Boltzmann Surface Area Method. *Mol. Inf.* **2012**, 31, 114-122.

[23] Stoll, V.; Stewart, K. D.; Maring, C. J.; .Muchmore, S.; Giranda, V.; Gu, Y. Y.; Wang, G.; Chen, Y. W.; Sun, M. H.; Zhao, C.; Kennedy, A. L.; Madigan, D. L.; Xu, Y. B.; Saldivar, A.; Kati, W.; Laver, G.; Sowin, T.; Sham, H. L.; Greer, J.; Kempf, D.. Influenza neuraminidase inhibitors: structure-based design of a novel inhibitor series. *Biochemistry*. **2003**. 42. 718-727.

[24] Hou, T. J.; Wang, J. M.; Li, Y. Y.; Wang, W. Assessing the Performance of the MM/PBSA and MM/GBSA Methods. 1. The Accuracy of Binding Free Energy Calculations Based on Molecular Dynamics Simulations. *J. Chem. Inf. Model*. **2011**, 51, 69-82.

Insert Table of Contents artwork here

A series of novel neuraminidase inhibitors containing the scaffold of N'-benzylidene benzohydrazone were designed and synthesized based on virtual screening.